

(本试剂盒仅供体外研究使用，不用于临床诊断!)

产品货号：E-BC-K881-M

产品规格：48T(16 samples)/96T(40 samples)

检测仪器：酶标仪(590-600 nm)

Elabscience®细胞亚铁比色法测试盒

Cell Ferrous Iron Colorimetric Assay Kit

使用前请仔细阅读说明书。如果有任何问题，请通过以下方式联系我们：

电话：400-999-2100

邮箱：biochemical@elabscience.cn

网址：www.elabscience.cn

具体保质期请见试剂盒外包装标签。请在保质期内使用试剂盒。

联系时请提供产品批号(见试剂盒标签)，以便我们更高效地为您服务。

用途

本试剂盒适用于检测细胞样本中亚铁的含量。

检测原理

铁是生物体内重要的金属元素之一，具有重要的生理作用。亚铁离子是血红素和血红蛋白中的关键元素，同时也在许多生化反应中起到重要作用。样本中的亚铁离子与探针结合，生成的物质在 593 nm 波长处有强吸收峰，在一定范围内其光密度值与亚铁离子浓度成线性相关。

提供试剂和物品

编号	名称	规格 1 (Size 1)(48 T)	规格 2 (Size 2)(96 T)	保存方式 (Storage)
试剂一 (Reagent 1)	缓冲液 (Buffer Solution)	45 mL×1 瓶	35 mL×2 瓶	2-8°C 避光 保存 6 个月
试剂二 (Reagent 2)	对照液 (Control Solution)	5 mL×1 瓶	10 mL×1 瓶	2-8°C 避光 保存 6 个月
试剂三 (Reagent 3)	显色液 (Chromogenic Solution)	5 mL×1 瓶	10 mL×1 瓶	2-8°C 避光 保存 6 个月
试剂四 (Reagent 4)	1 mmol/L 铁标准品 (1 mmol/L Iron Standard)	2 mL×1 瓶	2 mL×1 瓶	2-8°C 避光 保存 6 个月
	96 孔酶标板	1 板		
	96 孔覆膜	2 张		
	样本位置标记表	1 张		

说明：试剂严格按上表中的保存条件保存，不同测试盒中的试剂不能混用。

对于体积较少的试剂，使用前请先离心，以免量取不到足够量的试剂。

所需自备物品

仪器：酶标仪(590-600 nm，最佳检测波长为 593 nm)

试剂准备

① 检测前，试剂盒中的试剂平衡至室温。

② 100 $\mu\text{mol/L}$ 铁标准品的配制：

取100 μL 试剂四，与900 μL 试剂一混合均匀。按需配置，现配现用。

③ 不同浓度标准品的稀释：

编号	①	②	③	④	⑤	⑥	⑦	⑧
标准品浓度($\mu\text{mol/L}$)	0	5	10	15	20	25	30	35
100 $\mu\text{mol/L}$ 标准品(μL)	0	25	50	75	100	125	150	175
试剂一(μL)	500	475	450	425	400	375	350	325

样本准备

① 样本处理

细胞样本:取收集好的细胞按约每 1×10^6 个细胞加入 0.2 mL 的试剂一,混匀后放置在冰盒上裂解 10 min,再 $15000 \times g$ 离心 10 min,取上清液备用。

② 样本的稀释

在正式检测前,需选择2-3个预期差异大的样本稀释成不同浓度进行预实验,根据预实验的结果,结合本试剂盒的线性范围: $0.4-35 \mu\text{mol/L}$,请参考下表稀释(仅供参考):

样本	稀释倍数	样本	稀释倍数
HepG2 细胞	不稀释	molt-4 细胞	不稀释
Jurkat 细胞	不稀释	HEL 细胞	不稀释

注: 稀释液为试剂一。

实验关键点

- ① 为避免污染试剂三,可用 EP 管将试剂三分装一部分使用。
- ② 在使用移液枪向酶标板中加入液体时避免气泡产生。
- ③ 尽量选取新鲜的细胞样本进行实验。

操作步骤

- ① 标准孔：取 80 μL 不同浓度标准品，分别加入酶标板相应孔中。
测定孔：取 80 μL 待测样本，加入酶标板相应孔中。
对照孔：取 80 μL 待测样本，加入酶标板相应孔中。
- ② 向对照孔中加入 80 μL 试剂二。
- ③ 向测定孔、标准孔中加入 80 μL 试剂三。
- ④ 混匀，37 $^{\circ}\text{C}$ 孵育 10 min。
- ⑤ 在酶标仪 593 nm 处测定各孔 OD 值。

操作表

	标准孔	对照孔	测定孔
不同浓度标准品(μL)	80	--	--
待测样本(μL)	--	80	80
试剂二(μL)	--	80	--
试剂三(μL)	80	--	80
37 $^{\circ}\text{C}$ 孵育 10 min，在酶标仪 593 nm 处测定各孔 OD 值。			

结果计算

标准品拟合曲线: $y = ax + b$

细胞样本(以细胞个数进行计算):

$$\text{Fe}^{2+} \text{含量} \text{ (nmol/10}^6\text{)} = \frac{\Delta A - b}{a} \div \frac{N}{V} \times f$$

注解:

y: 标准品 OD 值-空白 OD 值(标准品浓度为 0 时的 OD 值)

x: 标准品的浓度

a: 标曲的斜率

b: 标曲的截距

ΔA : 样本的绝对 OD 值(测定孔 OD 值-对照孔 OD 值)

N: 用于裂解的细胞样本数量/ 10^6

V: 细胞样本处理时试剂一加入量(mL)

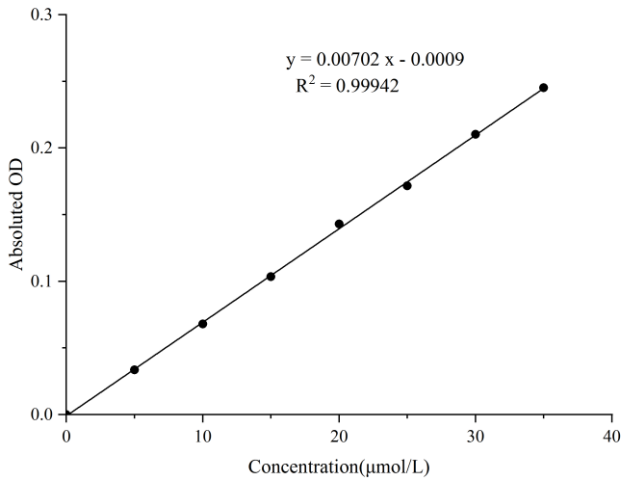
f: 样本加入检测体系前的稀释倍数

附录1 关键数据

1. 技术参数

检测范围	0.4-35 $\mu\text{mol/L}$	平均批间差	1.5 %
灵敏度	0.4 $\mu\text{mol/L}$	平均批内差	1.3 %
平均回收率	99 %		

2. 标准曲线(数据仅供参考)



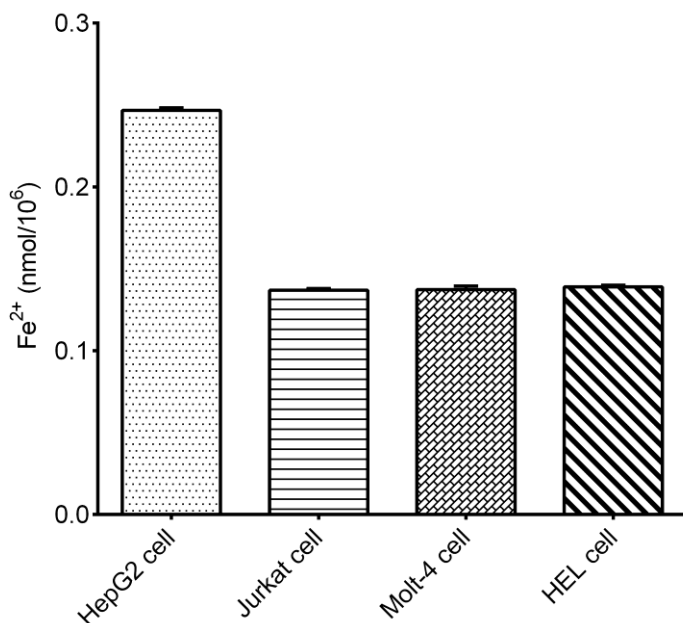
附录2 实例分析

例如检测HepG2细胞(数据仅供参考):

取 1.5×10^6 个HepG2细胞加入0.2 mL试剂一, 经过样本处理后, 取80 μ L按操作表进行检测, 其结果如下: 标准曲线: $y = 0.00605x + 0.0009$, 测定孔平均OD值为0.055, 对照孔平均OD值为0.043, 亚铁离子含量计算结果为:

$$\text{Fe}^{2+}\text{含量} \left(\frac{\text{nmol}}{10^6} \right) = \frac{0.055 - 0.043 - 0.0009}{0.00605} \div \frac{1.5}{0.2} = 0.24 \text{ nmol}/10^6$$

按照说明书操作, HepG2细胞(约 1.5×10^6 个细胞加入0.2 mL试剂一)、Jurkat、Molt-4、HEL细胞(约 1×10^6 个细胞加入0.2 mL试剂一)中的亚铁含量(如下图):



附录3 问题答疑

问题	可能原因	建议解决方案
无法检测出样本含量	细胞中 Fe^{2+} 含量低于检出限	增加细胞个数
复孔差异大	样本中有固体杂质未去除干净	延长离心时间
	酶标板孔中有气泡	加液时将枪头贴近孔内壁缓慢加入

声明

1. 试剂盒仅供研究使用，如将其用于临床诊断或任何其他用途，我公司将不对因此产生的问题负责，亦不承担任何法律责任。
2. 实验前请仔细阅读说明书并调整好仪器，严格按照说明书进行实验。
3. 实验中请穿着实验服并戴乳胶手套做好防护工作。
4. 试剂盒检测范围不等同于样本中待测物的浓度范围。如果样品中待测物浓度过高或过低，请对样本做适当的稀释或浓缩。
5. 若所检样本不在说明书所列样本类型之中，建议先做预实验验证其检测有效性。
6. 最终的实验结果与试剂的有效性、实验者的相关操作以及实验环境等因素密切相关。本公司只对试剂盒本身负责，不对因使用试剂盒所造成的样本消耗负责，使用前请充分考虑样本可能的使用量，预留充足的样本。

附录4 客户发表文献

1. Du S, Zhou N, Xie G, et al. Surface-engineered triboelectric nanogenerator patches with drug loading and electrical stimulation capabilities: Toward promoting infected wounds healing[J]. *Nano Energy*, 2021, 85:106004. IF:17.087
2. Bartolini D, Arato I, Mancuso F, et al. Melatonin modulates Nrf2 activity to protect porcine pre-pubertal Sertoli cells from the abnormal H₂O₂ generation and reductive stress effects of cadmium. *J Pineal Res.* 2022;73 (1):e12806. IF:13.007
3. Yang Z, Wang J, Ai S, et al. Self-generating oxygen enhanced mitochondrion-targeted photodynamic therapy for tumor treatment with hypoxia scavenging[J]. *Theranostics*, 2019, 9(23): 6809. IF:11.556
4. Wan Q, Cao R, Wen G, et al. Sequential use of UV-LEDs irradiation and chlorine to disinfect waterborne fungal spores: Efficiency, mechanism and photoreactivation[J]. *Journal of Hazardous Materials*, 2022, 423:127102-. IF:10.588
5. Tian J, Wang L, Hui S, et al. Cadmium accumulation regulated by a rice heavy-metal importer is harmful for host plant and leaf bacteria. *J Adv Res.* 2022. IF:10.479
6. Jg A, Jie S B, Jy B, et al. Comparative toxicity reduction potential of UV/sodium percarbonate and UV/hydrogen peroxide treatments for bisphenol A in water: An integrated analysis using chemical, computational, biological, and metabolomic approaches[J]. *Water Research*, 2020, 190. IF:9.702
7. Yang X X, Xu X, Wang M F, et al. A nanoreactor boosts chemodynamic therapy and ferroptosis for synergistic cancer therapy using molecular amplifier dihydroartemisinin[J]. *Journal of Nanobiotechnology*, 2022, 20(1):1-19. IF:9.464
8. Liu Z, Liu X, Yang Q, et al. Neutrophil membrane-enveloped nanoparticles for the amelioration of renal ischemia-reperfusion injury in mice[J]. *Acta Biomaterialia*, 2020, 104: 158-166. IF:8.947
9. Huang S, Le H, Hong G, et al. An all-in-one biomimetic iron-small interfering RNA nanoplatfrom induces ferroptosis for cancer therapy. *Acta Biomater.* 2022;148:244-257. IF:8.291
10. Alharbi YM, Sakr SS, Albarrak SM, et al. Antioxidative, Antidiabetic, and Hypolipidemic Properties of Probiotic-Enriched Fermented Camel Milk Combined with *Salvia officinalis* Leaves Hydroalcoholic Extract in Streptozotocin-Induced Diabetes in Rats. *Antioxidants (Basel)*. 2022;11 (4):. IF:7.675
11. Wang H, Huang Q, Zhang Z, et al. Transient post-operative overexpression of CXCR2 on

- monocytes of traumatic brain injury patients drives monocyte chemotaxis toward cerebrospinal fluid and enhances monocyte-mediated immunogenic cell death of neurons in vitro[J]. *Journal of Neuroinflammation*, 2022. IF:7.573
12. Liu P, Yin Z, Chen M, et al. Cytotoxicity of adducts formed between quercetin and methylglyoxal in PC-12 cells[J]. *Food Chemistry*, 2021, 352(2):129424. IF:7.514
 13. Adhikari B, Adhikari M, Ghimire B, et al. Cold plasma seed priming modulates growth, redox homeostasis and stress response by inducing reactive species in tomato (*Solanum lycopersicum*)[J]. *Free Radical Biology and Medicine*, 2020, 156: 57-69. IF:7.376
 14. Zhao X, Wang C, Dai S, et al. Quercetin Protects Ethanol-Induced Hepatocyte Pyroptosis via Scavenging Mitochondrial ROS and Promoting PGC-1 α -Regulated Mitochondrial Homeostasis in L02 Cells. *Oxid Med Cell Longev*. 2022;2022:4591134. IF:7.31
 15. Chagas TQ, Freitas N, Montalvão MF, Nobrega RH, Machado MRF, Charlie-Silva I, Araújo APDC, Guimarães ATB, Alvarez TGDS, Malafaia G. Multiple endpoints of polylactic acid biomicroplastic toxicity in adult zebrafish (*Danio rerio*)[J]. *Chemosphere*. 2021 Aug;277:130279. IF:7.086
 16. Mlindeli Gamede, Lindokuhle Mabuza, Phikelelani Ngubane, et al. Preventing the onset of diabetes-induced chronic kidney disease during prediabetes: The effects of oleanolic acid on selected markers of chronic kidney disease in a diet-induced prediabetic rat model[J]. *Biomedicine & Pharmacotherapy*. 2021 Jul;139:111570. IF:6.529
 17. Yang H, Zhu Y, Ye Y, et al. Nitric oxide protects against cochlear hair cell damage and noise-induced hearing loss through glucose metabolic reprogramming[J]. *Free radical biology & medicine*, 2021. IF:6.525
 18. Rao M J, Xu Y, Tang X, et al. CsCYT75B1, a Citrus CYTOCHROME P450 Gene, Is Involved in Accumulation of Antioxidant Flavonoids and Induces Drought Tolerance in Transgenic Arabidopsis[J]. *Antioxidants & Redox Signaling*, 2020, 9(2):161. IF:6.313
 19. Liou G G, Hsieh C C, Lee Y J, et al. N-Acetyl Cysteine Overdose Inducing Hepatic Steatosis and Systemic Inflammation in Both Propacetamol-Induced Hepatotoxic and Normal Mice[J]. *Antioxidants*, 2021, 10(3):442. IF:6.312
 20. Wang Y, Chi H, Xu F, et al. Cadmium chloride-induced apoptosis of HK-2 cells via interfering with mitochondrial respiratory chain[J]. *Ecotoxicology and Environmental Safety*, 2022, 236:113494-. IF:6.233
 21. Obaid QA, Al-Shammari AM, Khudair KK. Glucose Deprivation Induced by Acarbose and Oncolytic Newcastle Disease Virus Promote Metabolic Oxidative Stress and Cell

Death in a Breast Cancer Model. *Front Mol Biosci.* 2022;9:816510. IF:6.113

22. Abdel-Wahab BA, Walbi IA, Albarqi HA, Ali FEM, Hassanein EHM. Roflumilast protects from cisplatin-induced testicular toxicity in male rats and enhances its cytotoxicity in prostate cancer cell line. Role of NF- κ B-p65, cAMP/PKA and Nrf2/HO-1, NQO1 signaling[J]. *Food Chem Toxicol.* 2021 May;151:112133. IF:6.023
23. Aljutaily T. Evaluating the Nutritional and Immune Potentiating Characteristics of Unfermented and Fermented Turmeric Camel Milk in Cyclophosphamide-Induced Immunosuppression in Rats. *Antioxidants (Basel).* 2022;11 (4):. IF:5.952
24. Jabbari N, Nawaz M, Rezaie J. Ionizing Radiation Increases the Activity of Exosomal Secretory Pathway in MCF-7 Human Breast Cancer Cells: A Possible Way to Communicate Resistance against Radiotherapy[J]. *International Journal of Molecular Sciences*, 2019, 20(15):3649-. IF:5.923
25. Shanmugarajan D, Girish C, Harivenkatesh N, et al. Antihypertensive and pleiotropic effects of *Phyllanthus emblica* extract as an add-on therapy in patients with essential hypertension—A randomized double-blind placebo-controlled trial[J]. *Phytotherapy Research*, 2021. IF:5.878
26. Marzocco S, Fazeli G, Di Micco L, et al. Supplementation of Short-Chain Fatty Acid, Sodium Propionate, in Patients on Maintenance Hemodialysis: Beneficial Effects on Inflammatory Parameters and Gut-Derived Uremic Toxins, A Pilot Study (PLAN Study)[J]. *Journal of Clinical Medicine*, 2018. IF:5.688
27. Peng J, Pan J, Mo J, et al. MPO/HOCl Facilitates Apoptosis and Ferroptosis in the SOD1 G93A Motor Neuron of Amyotrophic Lateral Sclerosis. *Oxid Med Cell Longev.* 2022;2022:8217663. IF:5.604
28. Treadmill Exercise Alleviates Brain Iron Dyshomeostasis Accelerating Neuronal Amyloid- β Production, Neuronal Cell Death, and Cognitive Impairment in Transgenic Mice Model of Alzheimer's Disease[J]. *Molecular neurobiology*, 2021, 58(7):3208-3223. IF:5.59
29. Aboulhoda, B. E., Rashed, L. A., Ahmed, H., et al. Hydrogen sulfide and mesenchymal stem cells-extracted microvesicles attenuate LPS-induced Alzheimer's disease[J]. *Journal of Cellular Physiology*, 2021, 236(8):5994-6010 IF:5.546
30. Liu W, Jia H, Guan M, et al. Discovery of novel tubulin inhibitors targeting the colchicine binding site via virtual screening, structural optimization and antitumor evaluation. *Bioorg Chem.* 2022;118:105486. IF:5.508